ANALYSIS OF PHYSICAL MECHANISMS FOR THE DETECTION OF DNA IN CARBON NANOTUBE FIELD EFFECT TRANSISTORS FOR BIO-SENSING APPLICATIONS

BY

YANG ZHAO

THESIS

Submitted in partial fulfillment of the requirements
for the degree of Master of Science in Electrical and Computer Engineering
in the Graduate College of the
University of Illinois at Urbana-Champaign, 2011

Urbana, Illinois

Adviser:

Assistant Professor Gang Logan Liu

ABSTRACT

This thesis discusses the use of carbon nanotube field effect transistors as sensors for DNA. It proposes a band-gap modulation as the underlying physical mechanism by which detection occurs. Previous works have established that either Schottky–barrier modulation or electro–static gating are the most significant mechanisms, depending on the particular device. By analyzing field effect mobilities it can be seen that the band-gap modulation effect shows up in every device and can be a reliable means by which detection of hybridized DNA molecules can occur.

Dedicated to those who have lent me a bit of their lives.

ACKNOWLEDGMENTS

The author wishes to acknowledge Professor Logan Liu for all of his help and insight throughout the entire process, and Daniel Zuo for conversations and support.

TABLE OF CONTENTS

CHAPTER 1

INTRODUCTION

Since the rediscovery of carbon nanotubes (CNTs) by Iijima in 1991 [1], there has been a flurry of research investigating the properties and potential applications of this material. Many researchers have noted the excellent electronic properties of CNTs [2], [3] and have gone on to construct CNT field effect transistors [4]– [6]. The electronic properties of these transistors easily surpass those of traditional silicon FETs [4] and have led to intense speculation that CNTs could be the basis for the next generation of ultra fast and energy efficient electronics. Of particular interest are their excellent carrier mobilities, high current densities and one-dimensionality.

Aside from using CNT FETs to enhance computing performance, some researchers have been investigating the use of CNT FETs as DNA sensors [7]– [10]. One of the major motivations for this research is that traditional DNA detection methods using fluorescent dyes require preparation by a skilled technician and can take a relatively long time to complete [11]. FET based sensors promise much faster testing speeds, simpler operation and reduced cost, and there has been research in using even traditional silicon CMOS transistors [12]. The basic premise is to attach single strand DNA (ssDNA) to the gate oxide or CNT, which then only binds to its complement. When binding occurs, electrostatics of the DNA molecule interact with the FET and should result in a change in the electronic behavior of the device. The change in electronic behavior has been observed by several research groups,

but there is no consensus regarding what the detection mechanism is. In this work, an alternate approach is taken to analyze the data to shed new light on the topic by looking at field effect mobilities.

Before any serious discussion of the biosensing applications of carbon nanotube field effect transistors, it is worth outlining some fundamentals of their operation and fabrication especially as they relate to the properties that we will be examining. A carbon nanotube is essentially a sheet of graphene (carbon arranged in a hexagonal lattice) rolled up to form a tube. It can be semiconducting or metallic depending on the chirality [2]. Two thirds of the possible chiralities are semiconducting with the other third being metallic, and at the time of this writing there is not a well-developed method for controlling chirality during growth or for separating semiconducting from metallic nanotubes in a batch [13]. To prevent metallic nanotubes from bridging the channel and ruining the on/off ratio, the channel length is often quite large so that it takes several nanotubes in contact with each other to traverse the entire channel and lowers the chance of a completely metallic conduction path. The data that we examine come from devices that are fabricated roughly as follows. SiO_2 is grown on a wafer, metal contacts are patterned on, and CNTs are either grown using CVD before the contacts are made or deposited afterwards. Back-gated devices use the silicon wafer as the gate electrode while top-gated devices cover the device in an electrolyte and insert a gate electrode. In this configuration, the devices behave as FETs (generally p-type) and we can measure Id versus Vg at set drain voltages. Due to the random nature of the growth/deposition, it can be assumed that the electronic characteristics (except magnitude of current) can be adequately modeled by a single nanotube using the average parameters. Microfluidic channels, generally made from PMMA (polymethylmethacrylate), are some-

times mounted to the device. It should noted that CNT-FETs do sometimes exhibit ambipolar behavior due to interaction with oxygen in the atmosphere [4]. For use in biosensing, we take advantage of the CNT's compatibility with the carbon-based bio-molecules. This allows for single strand DNA to be attached to the CNT. The single strand DNA will then selectively bind only with its complement. When this binding occurs, there should be observable changes in the electronic properties of the device from when there is only the single strand DNA attached. Because of the selectivity of the binding, if the device is exposed to other non-complementary strands of DNA, binding will not occur and the behavior will be unchanged. This is the basic principle behind CNT-FET biosensors and an analysis based on carrier mobility is presented in the next section.

CHAPTER 2

PROCEDURES

2.1 Physical Mechanisms for Detection

Kaufman and Star summarized some of the work done and noted four mechanisms that are thought to be relevant and how they can be identified from Id-Vg plots [14]. The four mechanisms are electrostatic gating, mobility dampening, Schottky barrier modulation, and changes in the gate capacitance. Electro-static gating occurs due to the partial negative charge carried by DNA molecules and the accumulation of this charge can create an electric field that screens the electric field from the gate resulting in a shift in the device turn-on voltage. Schottky barriers form at the DNA-metal interface and the attachment of a DNA molecule can alter the height of this barrier, resulting in slightly higher conductance at one end and lower conductance at the other of a Id-Vg plot. A third possibility is mobility dampening where the chemisorbed and physisorbed DNA molecules serve to decrease carrier mobility, and this is reflected by overall lower conductance. Finally, the DNA can change the gate-capacitance of a top-gated device. The capacitance mechanism has not been observed to have any significant effect by any group. It should be noted that to really see the Schottky-barrier modulation behavior the gate voltage sweep must be wide enough for the device to show ambipolar behavior. In analyzing the data published by several research groups, we find that a strong argument can be made for a fifth process as the underlying

physical mechanism for detection.

2.2 Field Effect Mobilities in CNT Devices

Gui et al. presented data taken on back-gated devices and concluded that the detection mechanism is Schottky barrier modulation [9]. Tang et al. arrived at the same conclusion in their study using top-gated devices [8]. Heller et al. found that electro-static gating was the most significant mechanism [10]. These data sets were generated from very similar device configurations and their apparent disagreement warrants further study. We will examine all of these data sets through their field effect mobilities. Field effect mobility is given by the following equation as in [15], where μ is the field effect mobility, G is the conductance, L is the length of the channel, and ρ is the charge density.

$$\mu = \frac{GL}{\rho}$$

This can be found experimentally by extraction from Id–Vg data or calculated theoretically from device parameters. We extract the field effect mobilities of the data presented by several research groups and compare them to each other and against the simulations we have produced for their device configurations. Conductance is easily found from I_d, L is a device parameter, and ρ can be calculated from the gate capacitance.

The field effect mobilities are extracted from published I_d–V_g data by the following method. From the raw data, conductance is taken almost directly and the threshold voltage (V_t) is defined to be the intersection with the x-axis of the line tangent to the I_d–V_g curve at the point of peak transconductance. Once the threshold voltage is found, charge density is calculated from gate

capacitance and gate voltage. The definition of field effect mobility is then invoked and a plot versus charge density (or gate voltage beyond threshold) can be generated.

For a CNTFET the field effect mobility versus gate voltage/carrier concentration will adhere to the following trend. Once the gate voltage reaches threshold, the mobility will begin to increase. When the carrier energy is high enough that scattering into the second conduction band becomes possible we see the mobility peak and start to decrease. The location of this peak is determined by the band gap of the CNTs making up the channel of the device, which is related to the CNT's diameters. If all other parameters (dielectric material and thickness, device geometry) are held constant, then a larger band gap means the peak is farther from the threshold voltage. The absolute values of these mobilities generally range between 1,000 and 10,000 $V \cdot s/cm^2$, and some researchers have produced devices with even higher values [16]. This is an order of magnitude higher than silicon, making any changes that occur much easier to detect. The physical mechanisms will manifest in the following ways. Mobility dampening will lower the absolute mobility values. Gate voltage screening will not be reflected in the field effect mobility plots because we plot them starting at threshold so a change in the threshold will be subtracted out. Schottky barrier modulation will result in either a steeper or shallower curve at the onset of conduction (depending on if the barrier height is increased or decreased). Changes in the gate capacitance will appear to be a horizontally stretched version of the original graph. And lastly, band-gap modulation will manifest as a shift in the peak mobility.

2.3 Calculating Field Effect Mobility

All of the data examined was collected on devices that are back-gated and using SiO_2 as a dielectric. They are also all CNT-network FETs, meaning that the channel is made up of many CNTs. This will lower the on/off ratio of the devices because there will be some randomness in the diameters of the CNTs and it is possible to have metallic nanotubes that bridge the length of the channel. However, CNT network FETs will provide higher currents and are generally easier to fabricate. In order to simulate the field effect mobility for these devices, this work assumes that the channel is bridged by a single nanotube possessing the average characteristics of the network CNTs. The following parameters are important for the simulation and were matched to the actual device parameters where possible. Dielectric type and thickness determine the dielectric constant, which is used to calculate the gate capacitance (if back-gated). Channel length is used in the model as an upper bound for how far carriers can travel in the CNT. The band gap of the CNT is inversely related to the diameter and we use the data presented in the Kataura plots presented by S. Maruyama [17]. The diameter also plays a role in the maximum current that a CNT can carry; however, for these applications the devices are never pushed so far. The presence of a Schottky barrier is determined by the quality of the contact and the contact metal, the work function of carbon nanotubes is generally accepted to be roughly 5 eV [18], and good contacts have been obtained with both gold and palladium [19]. The devices are assumed to be operating at room temperature (300 K). For the specifics regarding the model that is used please refer to [20].

CHAPTER 3

DISCUSSION

3.1 Results

When interpreting the Id–Vg data, both Tang et al. [8] and Gui et al. [9] arrive at the same conclusion about Schottky barrier modulation. This work uses Gui et al.'s data set for its smaller hysteresis. Heller et al.'s [10] data simply does not sweep out far enough to include features of interest. Star et al.'s [7] data does show the same features in the Id–Vg that Heller et al. claim to be indicative of electrostatic gating. So we will be looking closely at the data from Gui et al. and Star et al.

Simulations of field effect mobility in a back-gated CNT FET for various diameters (band gaps) are shown in Figure 3.1. One can clearly see a non-monotonic behavior with a peak mobility. This peak occurs at roughly the point that the carriers enter the second conduction band. As the band-gap changes, one can see a shift in the location of the peak mobility as dictated by the theory. This shift is the key indicator that band-gap modulation has occurred. Figure 3.2 presents field effect mobilities extracted from data published by Star et al. [7]. The data is collected from a back-gated CNT network FET. One can clearly see the non-monotonic behavior showing that the device does indeed hit higher bands of conduction. We then turn our attention to the peak mobilities and note that the location shifts with the addition of ssDNA and hybridized DNA. The data shows that the hybridized

CNT enters the second conduction band at a smaller absolute gate voltage than the ssDNA CNT. This can be attributed to band-gap modulation. The negatively charge DNA molecules can also screen the gate voltage; however, this will cause the entire Id-Vg curve to shift uniformly, and we are plotting each curve from its threshold voltage so this effect does not show up in the field effect mobility plots.

Figure 3.3 shows data extracted from Gui et al. [9]. They fabricated a back-gated CNT network FET on a silicon/SiO_2 substrate. In this particular device the researchers configured it such that the DNA hybridization would occur close to the contacts. I have extracted field effect mobility from their data. As the gate voltage sweeps further beyond the threshold voltage one can see a clear non-monotonic behavior from the hybridized CNT. The sweeps do not go far enough to show the same for the ssDNA attached CNT and the bare CNT. However, the flattening out of the curves does suggest that they have hit their mobility peak before the end of the sweep. It can be clearly seen that with each additional piece of DNA the overall mobility of the device decreases. This is expected as the DNA physically and chemically interacts with the CNT and degrades the electronic performance. Another important feature is that the location of the peak mobility occurs at different gate voltages. As mentioned previously, the location of the peak is related to when carriers are injected into the second conduction band. A shift in the location can be due to changes in the band gap or capacitance of the gate. Gui et al. attribute the lowered conductance to Schottky barrier modulation and estimated a barrier height increase of roughly 16 meV from the bare device to the hybridized device. They also constructed another device where the regions near the contacts were passivated to ensure that any DNA hybridization that occurred would not happen at the contact region [9].

Figure 3.4 shows the field effect mobility information extracted from their data, and the non-monotonic behavior is much more pronounced than in the other device. The peaks shift, as we expect, from band-gap modulation. Figure 3.5 shows simulations of conductance using the methods outlined previously with the addition of a 16 meV Schottky barrier at the contact. The Schottky barrier is simulated using the WKB approximation for a triangular barrier. The simulation is performed for a variety of different diameters (and thus band gaps) and we see a monotonically increasing trend. Figure 3.6 shows the same simulations plotting field effect mobility versus charge density. The trend is decreasing and makes sense qualitatively as the presence of the Schottky barrier affects the device most at low gate voltages (charge densities) and dampens away the hump. The descending behavior is not seen in any of the experimental data. It should be noted that the monotonic behavior shown only occurs in some of the data extracted from Gui et al.

Figure 3.1 shows simulated field effect mobility; it should be noted that the location of the peak mobility shifts with changes in the band gap by the equivalent of roughly 1 V from $E_g = 0.28$ eV to 0.42 eV. In Figure 3.7 a simulation is run using the parameters from the sensor fabricated by Star et al. and then the band gap is adjusted to produce the second curve. The difference in magnitude between the simulated mobilities can be attributed to simplifying assumptions made in the model and to non-idealities in the device. We can clearly see the peak mobility shift roughly 1 to 1.5 V toward the threshold from the receptor-immobilized device to the fully hybridized device; this same shift is seen in the data in Figure 3.2. Both the simulation and the experimental data also show roughly a 20% decrease in mobility. Similar simulations could not be produced for Gui et al.'s data due to lack of information on some of the device parameters, but it should be re-iterated

that mobility peak shift indicative of band-gap modulation is clearly seen that data set as well.

3.2 Mobility Dampening

As mentioned previously, the magnitude of the field effect mobility noticeably decreases when ssDNA is added and again when the fully hybridized DNA is attached. The decrease is seen in every data set that we have examined and most attribute it to the DNA disrupting the carrier transport and thus decreasing the mobility and overall current. I attempted to model this by adding another scattering length to the simulation model, the reasoning being that the interaction between the DNA molecules and the CNT may cause localized scattering centers. The model used normally accounts for three different types of scattering: optical phonon emission and absorption, and acoustic phonon emission. With the addition of DNA molecules, a fourth type was added as a fitting parameter. By adjusting this additional mean free path directly, a good fit to the data could be found. However, in order to get a good fit, the mean free path suggested that the interaction between the DNA and the CNT only created 1-2 localized scattering centers over the length of the channel. This implies that the DNA-CNT interaction is not causing a scattering center at the point of interaction as over the length of the channel we expect much more than just two points of interaction [8]. We can conclude that although the addition of DNA does dampen the carrier mobility, the dampening is unlikely to be a result of the creation of localized scattering centers.

3.3 Figures

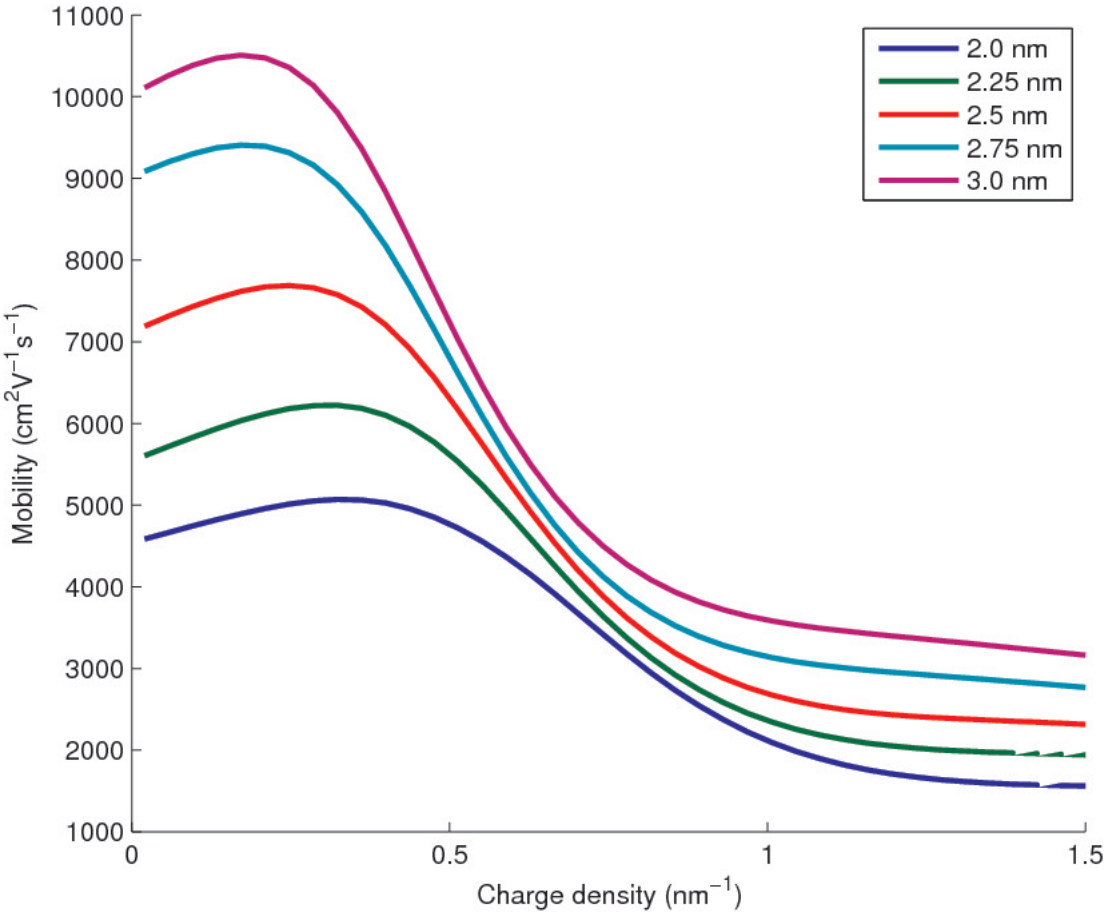

Figure 3.1: Simulations of idealized devices. Field effect mobility is plotted against carrier concentration. The simulations are performed for devices 5 μm in length, 100 nm of oxide, and good contacts. A range of CNT diameters is simulated.

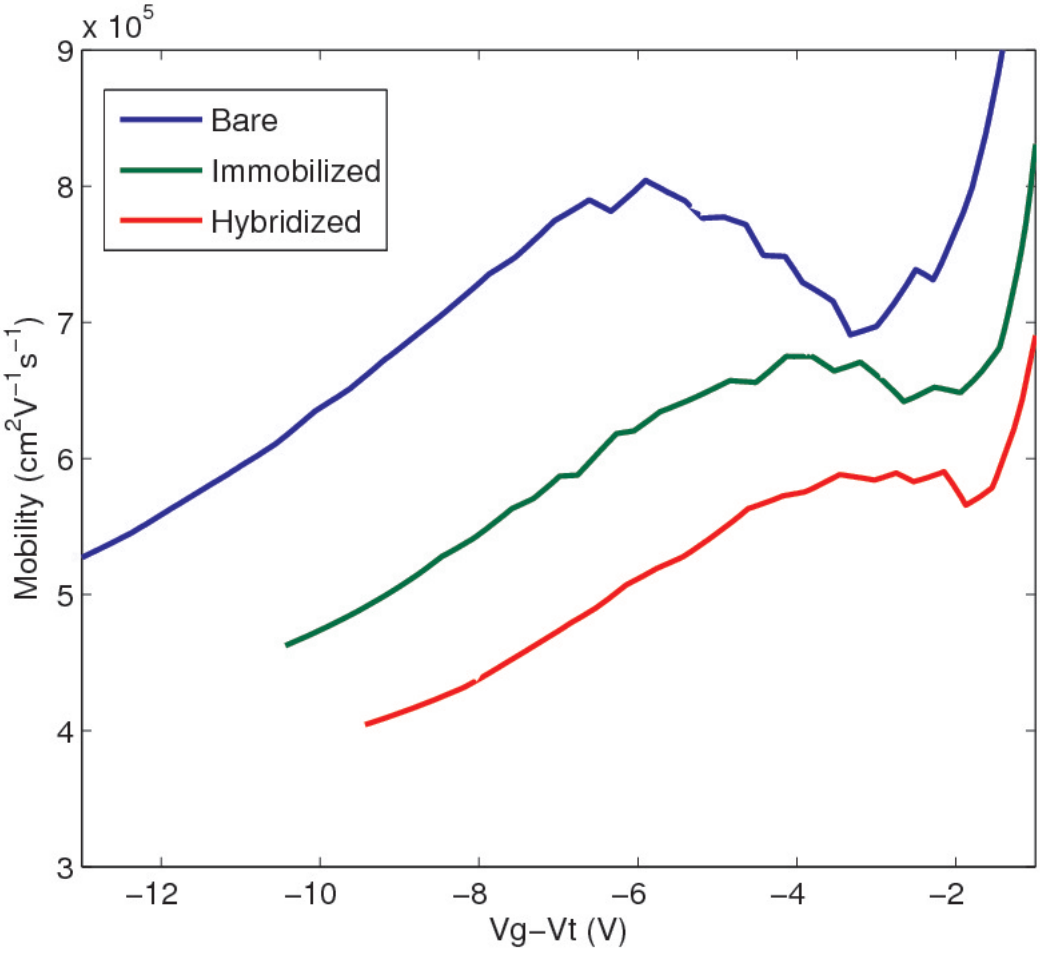

Figure 3.2: Field effect mobilities extracted from data published by Star et al. [7]. The blue curve (top) is of the bare device. The green curve (middle) is of the device with the probe (ssDNA) immobilized. The red curve (bottom) is of the device with fully hybridized DNA.

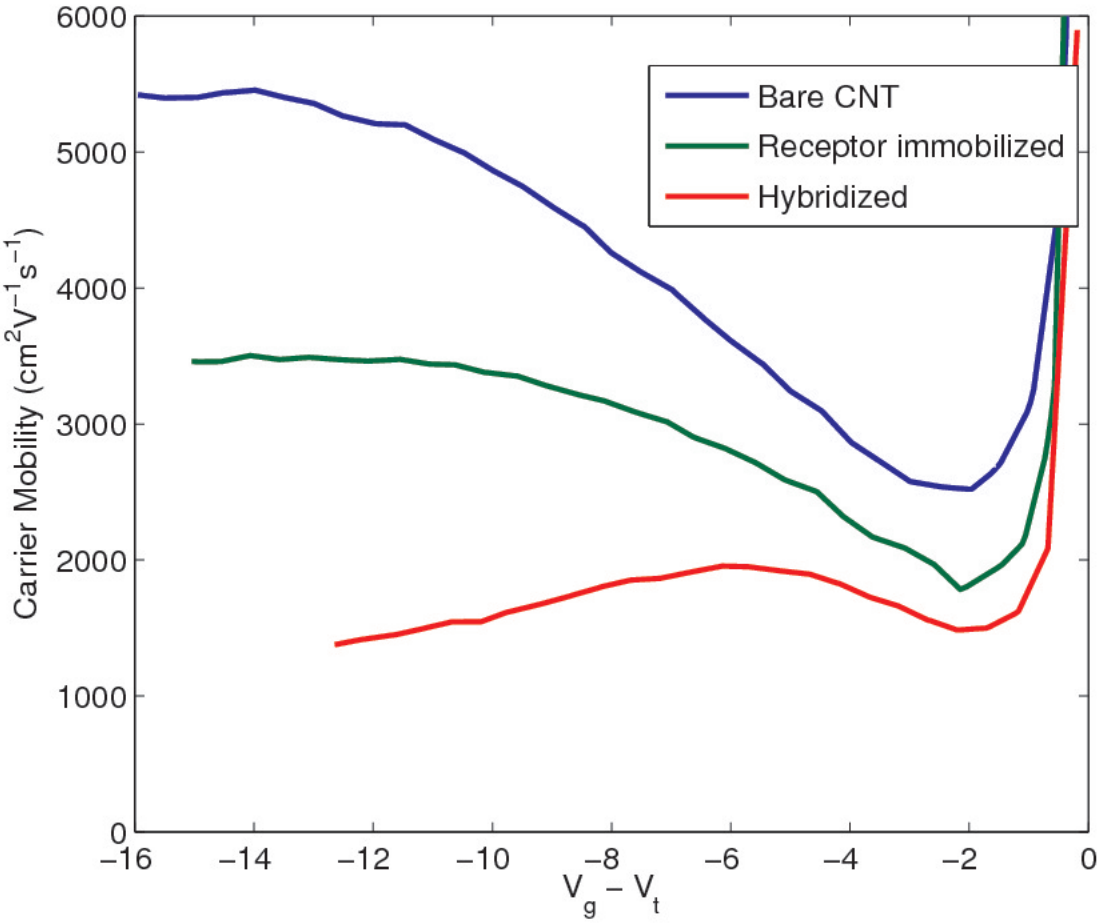

Figure 3.3: Field effect mobilities extracted from Gui et al. [9]. This device has the channel passivated so that the biomolecules would only interact with the region near the contacts. The blue curve (top) is of the bare device. The green curve (middle) is of the device with the probe (ssDNA) immobilized. The red curve (bottom) is of the device with fully hybridized DNA.

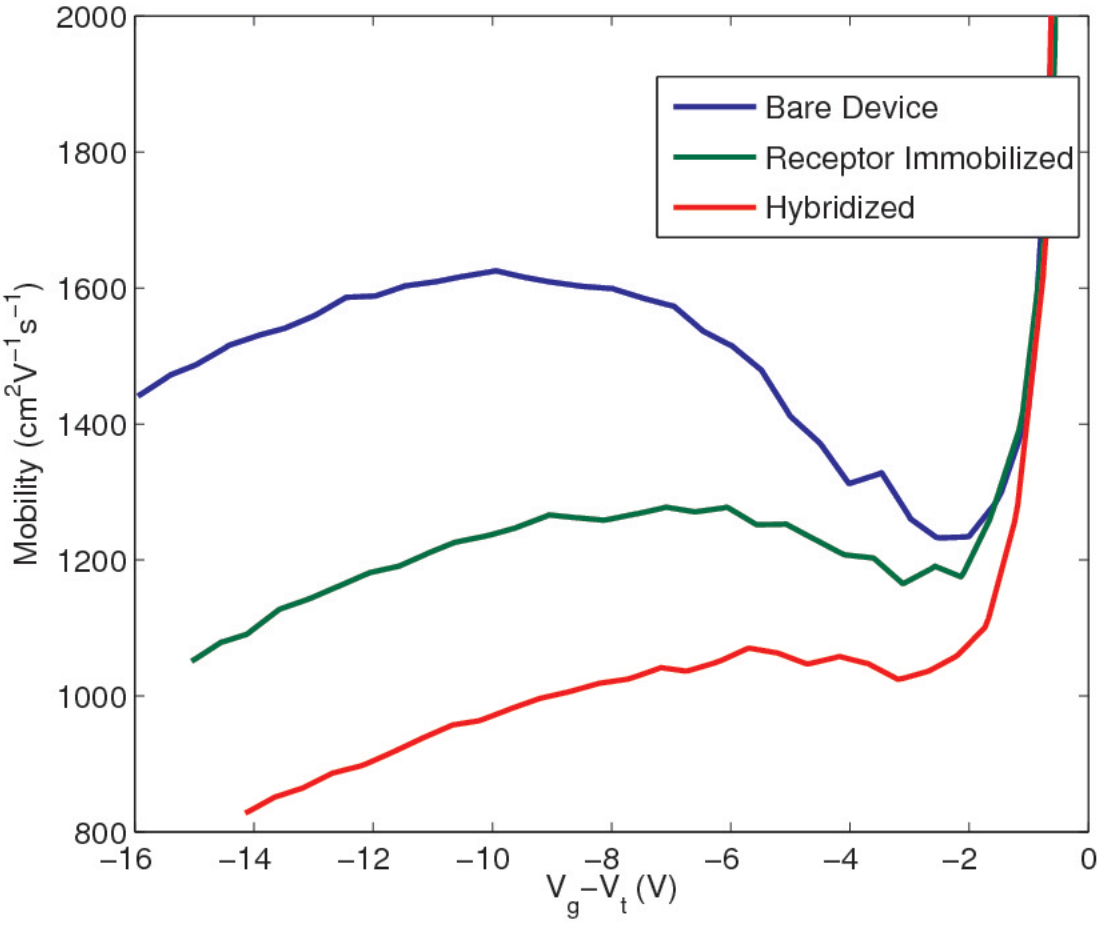

Figure 3.4: Field effect mobilities extracted from Gui et al. [9]. This device has the contact region passivated so that the biomolecules only interact with the device in the channel region. The blue curve (top) is of the bare device. The green curve (middle) is of the device with the probe (ssDNA) immobilized. The red curve (bottom) is of the device with fully hybridized DNA.

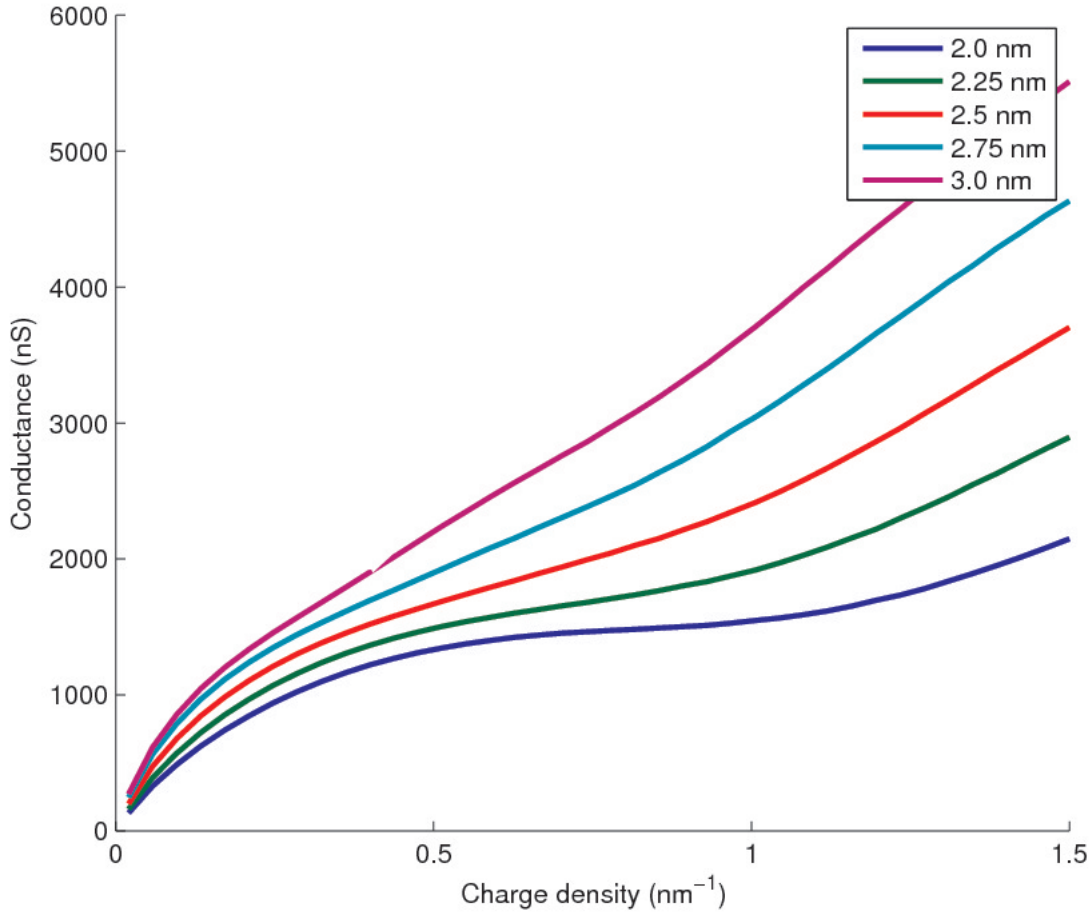

Figure 3.5: Simulations of conductance in CNT-FETs with various nanotube diameters with 16 meV Schottky barriers at the contacts.

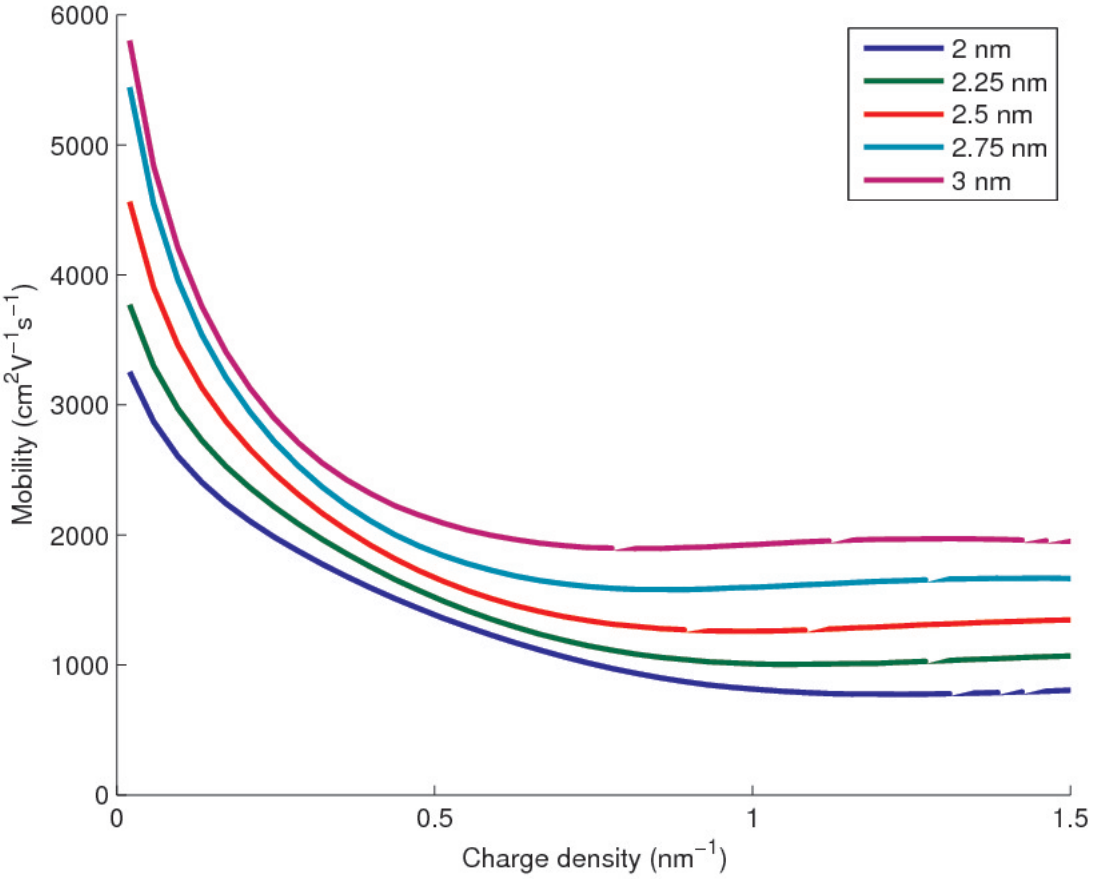

Figure 3.6: Simulations of field effect mobility in CNT-FETs with various nanotube diameters with 16 meV Schottky barriers at the contacts.

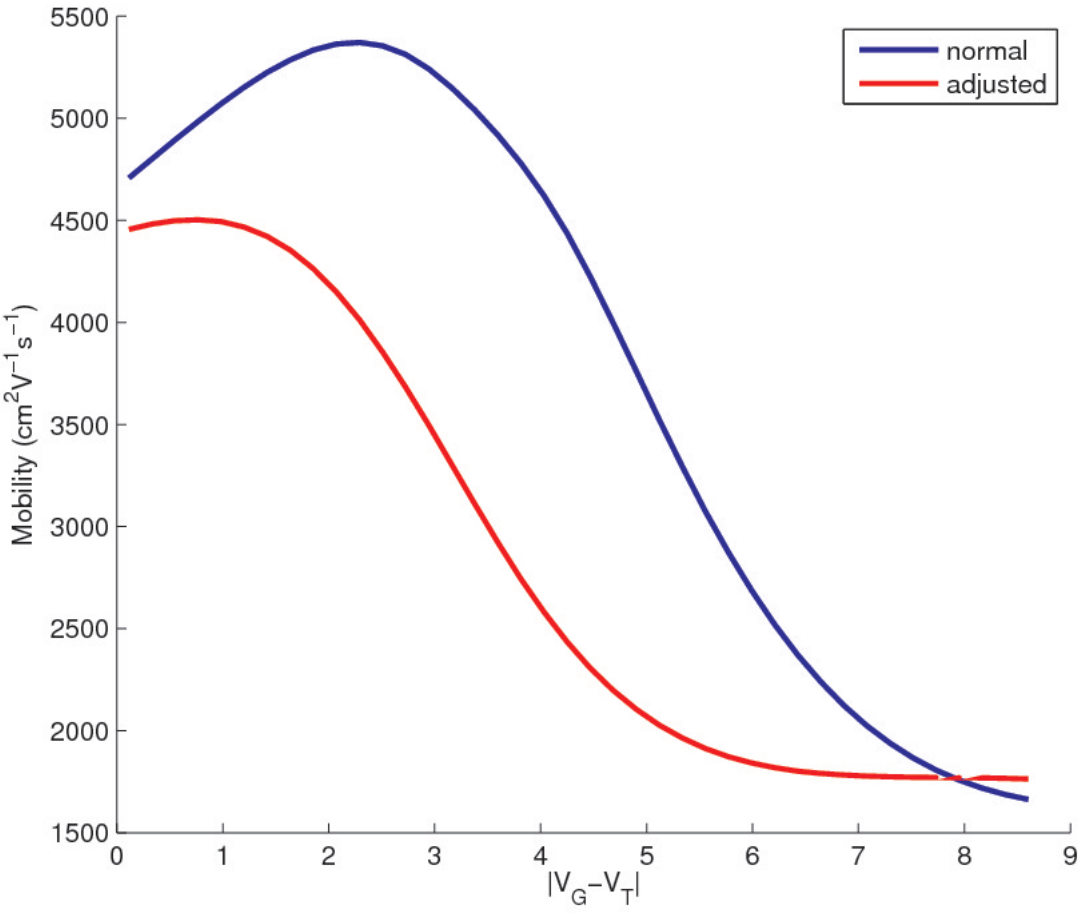

Figure 3.7: Simulations with device parameters matching those of Star et al. [7]. The blue curve (top) is the receptor immobilized device and the red curve (bottom) is the fully hybridized device. The hybridized curve is created solely by altering the band gap in the simulations.

CHAPTER 4

CONCLUSIONS

It is important to identify the underlying physical process by which detection occurs. By understanding what is happening, we can optimize devices to increase sensitivity, specificity, speed, detection accuracy, and noise tolerance. By looking at previously published data from different devices and examining them in the context of field effect mobility, it can be seen that current explanations based on the Schottky barrier modulation and electrostatic gating do not explain the entire story.

Based on the analysis of data published by Star et al. [7] and Gui et al. [9], it can be seen that the response can be explained by a combination of band-gap modulation and mobility dampening. We find that the detection mechanism is unlikely to be modulation of the Schottky barrier at the contact due to the retention of the non-monotonicity of the field effect mobility curve. Electrostatic gating could also be occurring, but the effect is only apparent in some of the data sets. By examining field effect mobility, the effect of band-gap modulation can be easily seen in the shift of the peak and appears in data sets where the Id–Vg analysis suggests two different physical mechanisms. Thus, a strong argument can be made that band-gap modulation is a significant physical process in the detection of DNA using carbon nanotube field-effect transistors.

CHAPTER 5

FUTURE WORK AND APPLICATIONS

5.1 Discussion

In order to verify and capitalize on the change in band gap, the following experimental device design is proposed (see Figure 5.1). It is based on a back-gated CNT-FET. The entire channel of the device will be passivated with a thin layer of poly(methyl methacrylate) (PMMA). DNA probes can be attached to plastic surfaces such as PMMA [21]. Presence of the complementary DNA strands will result in binding. The immobilized DNA will not be physically interacting with the CNT channel, so the mobility dampening effect should disappear. However, the charged nature of the DNA will still create an electric field and thus effectively isolate the band-gap modulation effect.

Most importantly, this configuration will isolate the band-gap modulation effect and we will be able to verify the strength of the effect and evaluate how feasible it is for use in bio-sensing applications. As a device schematic, this configuration has several advantages over current layouts. Current research is conducted on CNT-FET devices where the DNA is immobilized directly on the surface of the nanotube. This generally requires the nanotube to be exposed to the solution being tested. This exposes the CNT to everything in the solution, making it susceptible to contamination. In the PMMA passivated configuration, any stray particles in the solution being tested will rest

harmlessly on the PMMA and will not interact with the CNT unless they are charged. This extra tolerance is very desirable if this technology is ever to be used in the field where samples cannot undergo rigorous processing.

Another advantage of attaching DNA probes to PMMA instead of directly to the CNT channel is the potential for recycling the device. Since the PMMA is not electronically important to the operation of the device and acts as a sort of protective coating, the device can be treated to remove what is on the surface and re-attach more DNA probes as needed. In addition to protecting the CNTs, the PMMA adhesion layer can be patterned. This can be used to create microfluidic channels to aid in the delivery of the test sample.

There has been research done using nanowires [22] and CMOS technology [12], [23] and they all hold great promise for disease diagnostic applications. In order for this to become a viable technology, more experimental work needs to be done to verify the physical processes that occur and also improve on sensitivity, repeatability and yield. For CNT FET biosensors to become viable, there needs to be some more investigation into the fabrication techniques for these devices so that arrayed structures for testing many different sequences at the same time can be produced consistently.

Another avenue of future research would be to directly compare the CNT-FET based sensors to nanowire and CMOS based sensors and find which is the most effective and easiest to produce and integrate into modern healthcare. It is unlikely that all three technologies will become commercially viable as they all have the same goal of sensing specific bio-molecules with an electronic response.

The main application for these biosensors is, of course, in disease diagnostics. Many diseases can be diagnosed by the presence of specific bio-molecules or DNA sequences; sensors that can detect these molecules or sequences

can make identifying a patient's affliction much easier. CNT-based sensors have been developed for the detection of hepatitis B [24] and also for matrix metallopeptidase-9 and S-100B (the biomarkers present during a stroke) [25]. Traditionally this is done by chemical processes that require a skilled technician many hours to perform. With CNT-FET based biosensors, once a sample is placed on the chip, it can quickly and automatically determine which bio-molecules are present without the need for a highly trained technician. This has the potential to greatly lower the cost, in both time and money, of disease diagnostics and also increase its accessibility in poorer areas of the world.

5.2 Figure

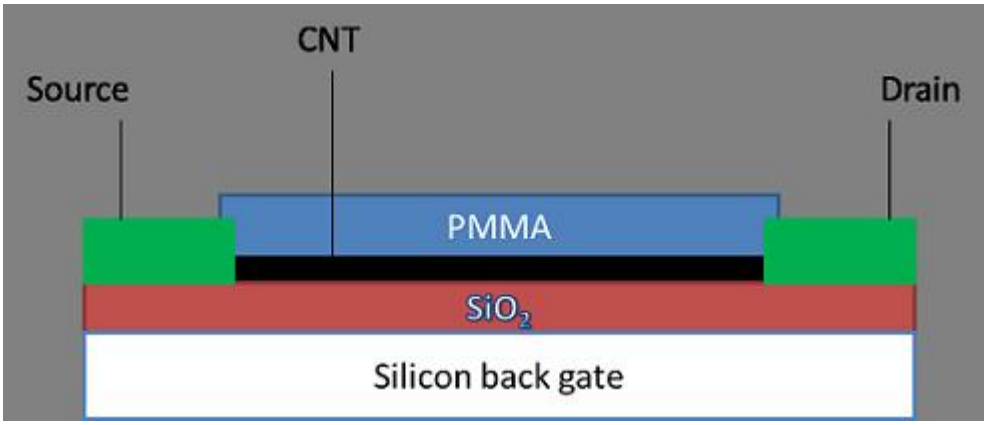

Figure 5.1: Cross-section of the proposed experimental device to verify and isolate the band-gap modulation effect. DNA probes would be attached to the PMMA layer above the CNT channel.

REFERENCES

[1] S. Iijima, "Helical microtubules of graphitic carbon," *Nature*, vol. 354, pp. 56–58, Nov. 1991.

[2] R. Saito, G. Dresselhaus, and M.S. Dresselhaus, *Physical Properties of Carbon Nanotubes*. London: Imperial College Press, 1998.

[3] M.S. Dresselhaus, G. Dresselhaus, and P. Avouris, *Carbon Nanotubes: Synthesis, Structure, Properties and Applications*. New York: Springer, 2001.

[4] P. Avouris, "Carbon nanotube electronics," *Chemical Physics*, vol. 281, pp. 429–445, Aug. 2002.

[5] J. Appenzeller, J. Knoch, R. Martel, V. Derycke, S.J. Wind, and P. Avouris, "Carbon nanotube electronics," *IEEE Trans. on Nanotechnology*, vol. 1, pp. 184–189, Dec. 2002.

[6] P.L. McEuen, M.S. Fuhrer, and H. Park, "Single-walled carbon nanotube electronics," *IEEE Trans. on Nanotechnology*, vol. 1, pp. 78–85, Mar. 2002.

[7] A. Star, E. Tu, J. Niemann, J.C.P. Gabriel, C.S. Joiner, and C. Valcke, "Label-free detection of DNA hybridization using carbon nanotube network field effect transistors," *Proceedings of the National Academy of Sciences*, vol. 103, pp. 921–926, Jan. 2006.

[8] X. Tang, S. Bansaruntip, N. Nakayama, E. Yenilmez, Y.I. Chang, and Q. Wang, "Carbon nanotube DNA sensor and sensing mechanism," *Nano Letters*, vol. 6, pp. 1632–1636, June 2006.

[9] E.L. Gui, L.J. Li, K. Zhang, Y. Xu, X. Dong, X. Ho, P.S. Lee, J. Kasim, Z.X. She, J.A. Rogers, and S.G. Mhaisalkar, "DNA sensing by field-effect transistors based on networks of carbon nanotubes," *Journal of the American Chemical Society*, vol. 129, pp. 14 427–14 432, Oct. 2007.

[10] I. Heller, A.M. Janssens, J. Mannik, E.D. Minot, S.G. Lemay, and C. Dekker, "Identifying the mechanism of biosensing with carbon nanotube transistors," *Nano Letters*, vol. 8, pp. 591–595, Dec. 2008.

[11] D. Proudnikov and A. Mirzabekov, "Chemical methods of DNA and RNA flourescent labeling," *Nucleic Acids Research*, vol. 24, pp. 4535–4542, Sep. 1996.

[12] M. Barbaro, A. Bonfiglio, L. Raffo, A. Alessandrini, P. Facci, and I. Barak, "A CMOS, fully integrated sensor for electronic detection of DNA," *IEEE Electron Device Letters*, vol. 24, pp. 4535–4542, Sep. 1996.

[13] D.W.H. Fam, A. Palaniappan, A.I.Y. Tok, B. Liedberg, and S.M. Moochhala, "A review on technological aspects influencing commercialization of carbon nanotube sensors," *Sensors and Actuators B: Chemical*, vol. 157, pp. 1–7, Apr. 2011.

[14] D. Kauffman and A. Star, "Electronically monitoring biological interactions with carbon nanotube field-effect transistors," *Chemical Society Reviews*, vol. 37, pp. 1197–1206, Apr. 2008.

[15] T. Fang, A. Konar, H. Xing, and D. Jena, "Mobility in semiconducting graphene nanoribbons: Phonon, impurity, and edge roughness scattering," *Physical Review B*, vol. 78, pp. 205 403–205 410, Oct. 2008.

[16] T. Durkop, S.A. Getty, E. Cobas, and M.S. Fuhrer, "Extraordinary mobility in semiconducting carbon nanotubes," *Nano Letters*, vol. 4, pp. 35–39, Dec. 2004.

[17] S. Maruyama, "Kataura-plot for resonant raman," 2002. [Online]. Available: http://www.photon.t.u-tokyo.ac.jp/ maruyama/kataura/kataura.html

[18] M. Shirashi and M. Ata, "Work function of carbon nanotubes," *Carbon*, vol. 39, pp. 1913–1917, Oct. 2001.

[19] Z. Chen, J. Appenzeller, J. Knoch, Y.M. Lin, and P. Avouris, "The role of metal–nanotube contact in the performance of carbon nanotube field–effect transistors," *Nano Letters*, vol. 30, pp. 1078–1080, Oct. 2009.

[20] Y. Zhao, A. Liao, and E. Pop, "Multiband mobility in semiconducting carbon nanotubes," *IEEE Electron Device Letters*, vol. 30, pp. 1078–1080, Oct. 2009.

[21] Y. Liu and C.B. Rauch, "DNA probe attachment on plastic surfaces and microfluidic hybridization array channel devices with sample oscillation," *Analytical Biochemistry*, vol. 317, pp. 76–84, Jan. 2003.

[22] F. Patolsky, G. Zheng, and C.M. Lieber, "Nanowire-based biosensors," *Analytical Chemistry*, vol. 78, pp. 4260–4269, July 2006.

[23] D.S. Kim, Y.T. Jeong, H.J. Park, J.K. Shin, P. Choi, J.H. Lee, and G. Lim, "An FET-type charge sensor for highly sensitive detection of DNA sequence," *Biosensors and Bioelectronics*, vol. 20, pp. 69–74, Mar. 2004.

[24] J. Oh, S. Yoo, Y.W. Chang, K. Lim, and K.H. Yoo, "Carbon nanotbe based biosensor for detection of hepatitis B," *Current Applied Physics*, vol. 9, pp. 229–231, July 2009.

[25] H.S. Lee, J.S. Oh, Y.W. Chang, Y.J. Park, J.S. Sin, and K.H. Yoo, "Carbon nanotube-based biosensor for detection of matrix metallopeptidase-9 and s-100b," *Current Applied Physics*, vol. 9, pp. 270–272, July 2009.